

# Sparse repulsive coupling enhances synchronization in complex networks

I. Leyva, I. Sendiña–Nadal, J.A. Almendral, and M.A.F. Sanjuán

*Dpto. de Ciencias de la Naturaleza y Física Aplicada,  
Universidad Rey Juan Carlos, c/ Tulipán s/n, 28933 Móstoles, Madrid, Spain*

(Dated: October 31, 2018)

Through the last years, different strategies to enhance synchronization in complex networks have been proposed. In this Letter, we show that the synchronization in a small-world network of attractively coupled non-identical neurons is strongly improved by adding a tiny fraction of phase-repulsive couplings. By a purely topological analysis that does not depend on the dynamical model, we link the emerging dynamical behavior to the structural properties of the sparsely coupled repulsive network.

PACS numbers: 87.19.La, 05.45.Xt

Synchronous oscillations in a large ensemble of oscillators are considered as one of the mechanisms in biological networks to transmit and code information, especially in the brain [1]. Recent experiments have pointed out the important role that the complex structure of connectivity has in this collective behavior [2], obtaining the signature of an underlying small-world (SW) network by indirect measures in neuronal culture samples [3] or using functional magnetic resonance imaging in humans [4]. Theoretically, several strategies have been developed with the aim of finding the best way to achieve synchronization in complex networks [5, 6, 7]. These approaches have mainly focused on the role that weighted links play in heterogeneous networks [8, 9, 10], shortest paths between nodes and clustering structure in SW networks [11], or the input degree each node receives regardless of the net structure [12].

Most of this research has been devoted to attractively coupled dynamical elements. However, it is known that biological networks combine different types of connections to improve synchronization and transmission performance, as in the case of the coexistence of excitatory and inhibitory synapses in the brain [13]. Nevertheless, little attention has been paid to the effect of repulsive coupling, or to the interaction between different types of coupling. The scarce literature addressing synchronization in repulsively coupled oscillators considers global or local coupling [14, 15], but the influence of the network structure is still an open question.

In addition, almost all the published work on synchronization in complex networks basically deals with arrays of identical units. However, heterogeneity of elements is an inherent feature present in natural systems which can be especially relevant in the dynamics of biological networks [16]. In this Letter, we explore the influence of the network topology on the dynamics of non-identical coupled units, when a small fraction of the links is phase-repulsive. We show that sparse repulsive links in a SW structure can induce a coherent oscillatory state when the equivalent SW composed of only attractive connections is not able to synchronize or even to activate the ensemble. Then, just by means of an analysis focused on the connectivity matrix, we link the emerging dynamical behavior to the structural

properties of the sparsely coupled repulsive network.

We study the dynamics of an ensemble of non-identical locally coupled Hodgkin-Huxley (HH) neurons [17] considered as spatially isopotential cells

$$C\dot{V}_i = I_i - I_i^{ion}(V_i, x_i) + d \sum_j \hat{L}_{ij} V_j \quad (1)$$

$$\dot{x}_i = \alpha_x(1 - x_i) - \beta_x x_i.$$

Here,  $V_i$  is the voltage across the membrane of neuron  $i$  of capacitance  $C$ , and  $\dot{x} = \{\dot{m}, \dot{n}, \dot{h}\}$  describes the gating of the ion channels.  $I_i^{ion} = g_{Na} m_i^3 h_i (V_i - V_{Na}) + g_K n_i^4 (V_i - V_K) + g_l (V_i - V_l)$  is the ionic current mainly carried by  $\text{Na}^+$  and  $\text{K}^+$  ions and other ionic currents through voltage dependent channels. These currents are driven by the voltage difference with respect to the equilibrium potentials  $V_{Na}$ ,  $V_K$  and  $V_l$  and the maximal ionic conductances  $g_{Na}$ ,  $g_K$  and  $g_l$ . Functions  $\alpha_x$  and  $\beta_x$  are voltage-dependent rate constants. Parameter values and functions are the standards in the literature [17, 18].  $I_i$  accounts for any external bias current, which has been chosen as a control parameter to introduce heterogeneity in the population by setting  $I_i$  uniformly distributed within the interval  $I_0 \pm \Delta I$ . The value  $I_0 = 9 \mu\text{A}/\text{cm}^2$  is fixed close to the point where an inverse Hopf bifurcation occurs,  $I_b = 9.5 \mu\text{A}/\text{cm}^2$ . This way, for the chosen  $\Delta I = 0.2$ , about 90% of the neurons stay around the silent state,  $V_{\text{rest}} = -65 \text{ mV}$ , while the rest will fire periodically.

The coupling structure in (1) is given by  $\hat{L}_{ij} = L_{ij}/k_i$ , where  $L_{ij}$  is the Laplacian matrix [19],  $k_i$  normalizes the connection strength by the number of incoming links to node  $i$ , and the coefficient  $d$  stands for the global coupling strength.

*Local coupling.*— Initially we consider the effect of a regular lattice on an ensemble of  $N$  neurons, both for fully phase-attractive and phase-repulsive coupling. The Laplacian matrix for the first case is  $L_{i,i\pm 1} = 1$ ,  $L_{ii} = -2$  and  $L_{ij} = 0$  otherwise. And, for the second one, it is  $L_{i,i\pm 1} = -1$ ,  $L_{ii} = 2$  and  $L_{ij} = 0$  otherwise.

Figure 1 shows the global mean firing rate (MFR) and its standard deviation  $\sigma_{\text{MFR}}$  as a function of  $d$  ranging from negative to positive values. The negative sign of  $d$  comes

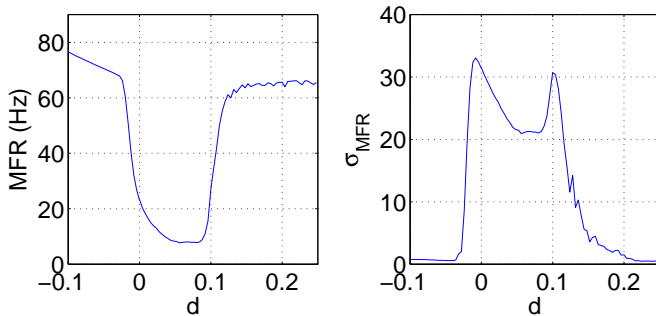


FIG. 1: Mean firing rate (left) and its standard deviation (right) for a  $N = 400$  regular array as a function of  $d$ , each point averaged over 100 realizations. The negative sign of  $d$  comes from the fully phase-repulsive connection matrix.

from the fully phase-repulsive connection matrix. When  $d > 0$  is large enough, the system is frequency entrained to a phase synchronization state. Equivalently, for a sufficient  $d < 0$ , the system reaches an anti-phase synchronization state. It can be noted from Fig. 1 that the entrainment with negative couplings is achieved for smaller absolute values of  $d$  compared to the case with positive ones. This indicates that a phase-repulsive coupling is more effective to activate and entrain the whole network. Many biological systems exhibit this kind of repulsive coupling when their dynamical units are in competition with each other. Known examples are the inhibitory coupling present in neuronal circuits associated to a synchronized behavior in central pattern generators [20] or calcium oscillations in epileptic human astrocyte cultures [21].

*Non local random coupling.*— Our main interest is to explore the influence of a SW-like connection topology in the activation and synchronization of the network. From the results obtained in the previous section, we know that a small positive coupling strength is less efficient than a negative coupling to activate and synchronize the whole network. Taking this into account, we consider now the possibility of non-local couplings both positive and repulsive. The global coupling strength is fixed to  $d = 0.1$ , i.e., within the unsynchronized regime for local positive coupling as shown in Fig. 1. The Laplacian matrix  $L$  is modeled now by keeping the regular short-range connections positive,  $L_{i,i\pm 1} = +1$ , and by randomly adding (rather than rewiring) a fraction  $p$  of the  $(N-1)(N-2)/2$  possible long-range links, being negative with probability  $p_n$ .

Figure 2 shows space-time plots of the voltage variable through the whole array for different probabilities  $p$  and  $p_n$ . As expected, in the absence of long-range connections, few more than the initial 10% of the neurons is firing for the chosen coupling strength  $d$ , i.e., the array is not even activated as shown in Fig. 2(a). When long-range links are included, the first observation is that for any  $p$ , a minimum fraction of the new added links needs to be repulsive in order to increase the activity of the network. This becomes

evident when comparing Fig. 2(b) with Figs. 2(c)-(e). In Fig. 2(b) the activity generated by the 10% of initially active neurons is reduced, or even annihilated, when all long-range connections are attractive ( $p_n = 0$ ). However, the scenario completely changes when, for the same  $p$ , some of the shortcuts are repulsive ( $p_n > 0$ ) as in Figs. 2(c)-(e) where self-sustained electrical activity emerges for nonzero  $p_n$ . In addition, we observe the existence of optimal probabilities  $p$  and  $p_n$  for which the collective oscillation becomes maximally phase-coherent. This fact can be observed by comparing Fig. 2(c), where  $p$  and  $p_n$  are optimal, and Fig. 2(d) where  $p_n$  is the same but  $p$  is slightly higher.

To study quantitatively how the dynamics is affected by  $p$  and  $p_n$ , we measure the MFR of the network and the standard deviation of the global electrical voltage,  $V(t) = \sum_{i=1}^N V_i(t)$ , obtained as  $\sigma_V = \sqrt{\langle V^2(t) \rangle - \langle V(t) \rangle^2}$ . While the MFR gives us an estimation of how much the network is activated, the  $\sigma_V$  defines how coherent is the activity of the entire network. If the network is fully activated, the MFR approaches to a rate of around 70 Hz, whereas  $\sigma_V$  is maximal if this activity is synchronized.

We have plotted in Fig. 3 both the MFR and the  $\sigma_V$  as a function of the probability  $p$  for different values of  $p_n$ . The signature of a network resonance both in  $p$  and  $p_n$  is clear from this figure: the frequency entrainment increases and phase synchronization is maximally enhanced for the optimal values  $p = p_c$  and  $p_n \approx 0.3$ . The probability  $p_c$  depends slightly on  $p_n$ , shifting to higher  $p$  as  $p_n$  increases, but remaining very small. The interplay between topology and dynamics becomes evident when we observe that the critical link probability depends strongly on the size ensemble as  $p_c \propto \ln(N)/N$ , i.e., coincides with the birth of the giant connected component (GCC) when only the random part of the network is considered.

Recently [10, 22], the method of the *master stability function* [23] has been successfully used to analyze whether the network structure has some bearing on the dynamics evolving on it. However, this approach requires the dynamical units to be identical (which is not our case) and, generally, the results are model-dependent. Therefore, in order to understand the influence of a complex connectivity, we use a purely structural analysis based on the properties of the matrix  $\hat{L}$ . To this purpose, we ignore the intrinsic dynamics of the neurons in Eq. (1), that is, we just consider  $\dot{\mathbf{V}} = d\hat{L}\mathbf{V}$ . Then, there is a basis in which  $V_i \approx \exp(d\lambda_i t)$ , where  $\lambda_i$  are the eigenvalues of  $\hat{L}$ . It is well known that all the eigenvalues of the Laplacian associated to a network with only attractive couplings are negative. However, when we add some repulsive connections,  $\hat{L}$  has positive and negative eigenvalues. We find that any set of initial states rapidly evolves into the subspace  $S^+$  associated to the positive eigenvalues within a time smaller than the characteristic temporal scale of the neuronal dynamics ( $\tau \approx 15$  ms).

To quantify the effect of  $S^+$ , we note that, for a

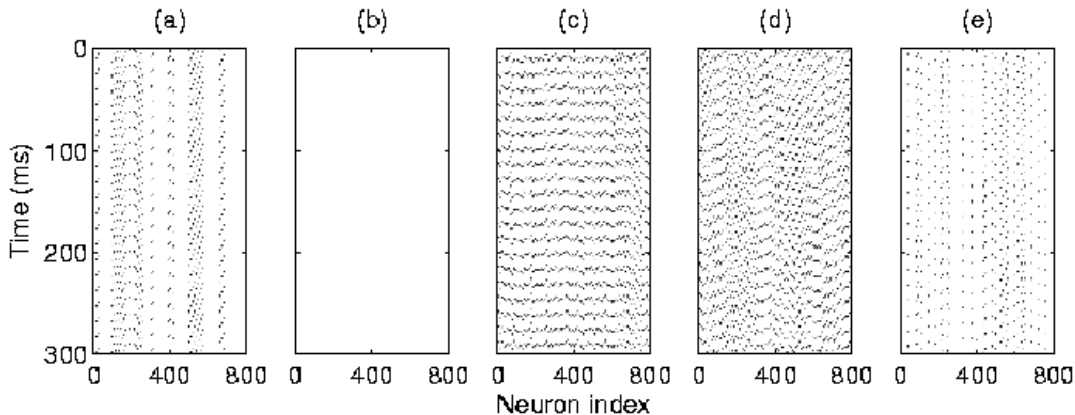


FIG. 2: Space-time plots of the neuron voltage for a  $N = 800$  HH units network, with  $\Delta I = 0.2$ ,  $d = 0.1$ , and different coupling connectivities: (a) Local coupling with  $p_n = 0$ ; (b) network with long range couplings,  $p = p_c = 0.0055$ , and  $p_n = 0$ ; (c)  $p = p_c = 0.0055$  and  $p_n = 0.3$ ; (d)  $p = p_c = 0.0055$  and  $p_n = 0.45$ ; (e)  $p = 0.015$  and  $p_n = 0.3$ .

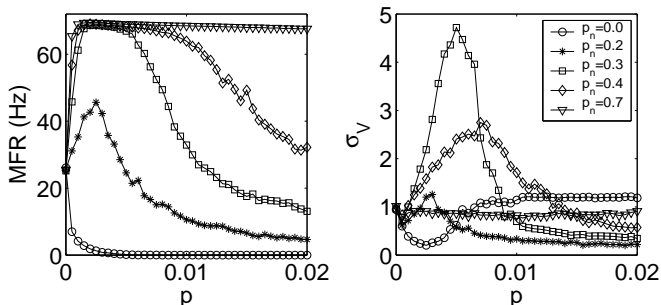


FIG. 3: MFR (left) and network coherence  $\sigma_V$  (right) as a function of  $p$  for several  $p_n$  in a  $N = 800$  network. Each point is averaged over 100 simulations, 1 s long (transients avoided), for different network and initial conditions realizations. Note that the legend applies to both figures.

given positive  $\lambda_i$ ,  $e^{d\lambda_i}$  is a measure of how much the system spreads into the subspace defined by the corresponding eigenvector. Then, the ratio  $e^{d\lambda_i t}/e^{d\lambda_{\max} t} = e^{d(\lambda_i - \lambda_{\max})t}$  measures how different is the evolution in that subspace with respect to the one where the system develops faster. By defining the geometric average  $g(t) = \prod_{i=1}^N e^{d(\lambda_i - \lambda_{\max})t/N} = e^{d(\langle \lambda \rangle - \lambda_{\max})t}$ , we can estimate the homogeneity of the evolution in  $S^+$  with a number in  $(0, 1]$ . A value close to 1 means the system evolves similarly in all dimensions of  $S^+$ , whereas a low  $g$  implies that its behavior is determined by those vectors with the largest associated eigenvalues.

We are interested in the behavior of  $g(t)$  as a function of  $p$  and  $p_n$ . As the shape of  $g(t)$  with  $p$  is not very sensitive to time, we fix  $t = d^{-1} \sim \tau$  to focus our study within the time scale of our dynamical unit (see Fig. 4(left)). We observe that  $g = g(\tau)$  presents a minimum at  $p_c$  which is lower for higher values of  $p_n$ , and whose position shifts to higher  $p$  as  $p_n$  increases, as observed in the numerical

simulations (Fig. 3(right)). This means that, for values of  $p$  far from  $p_c$ , i.e. where  $g \approx 1$ , the global dynamics is basically determined by only one positive eigenvalue,  $\mathbf{V}(t) = \mathbf{V}_0 \exp(\lambda t)$ . On the contrary, for values of  $p$  close to  $p_c$ , we need to consider not just one but several eigenvalues (the largest ones) to account for the global dynamics. Therefore, the intrinsic dynamics of the system is minimally constrained by the structure that arises around  $p_c$  due to the repulsive shortcuts.

To analyze if the previous structural result affects other dynamics imposed on it, we consider a discrete spin-like dynamics in which each node  $i$  has only two possible states  $s_i = \pm 1$ , with a probability  $p_-$  of being  $s_i = -1$ . Consequently, with the same link matrix  $\hat{L}$  studied above, node  $i$  receives an input  $h_i = \sum_j \hat{L}_{ij} s_j \in [-2, 2]$ . Hence, as other authors have pointed out [24, 25], these spin-like networks can be regarded as a pattern of the internal states and their evolution represent the global dynamics. Notice that the neighbor vertices linked repulsively contribute to the input with the opposite state. Then, in this model it is implicit that nodes linked with an attractive connection tend to follow the same evolution, whereas repulsive connection leads them to evolve differently.

We can prove analytically that the distribution of  $h_i$  presents two peaks:  $\mu_1 = -2p_- \sqrt{1 - 4p_n(1 - p_n)}$  and  $\mu_2 = 2(1 - p_-) \sqrt{1 - 4p_n(1 - p_n)}$ . Then, we choose to evolve the network according to the following local majority rule: the new state of node  $i$  is updated to  $s_i(n+1) = +1$  if  $h_i(n) > \mu_2$ ,  $s_i(n+1) = -1$  if  $h_i(n) < \mu_1$  and  $s_i(n+1) = s_i(n)$  otherwise (i.e., the vertex keeps its state).

When we average the mean state of nodes after a transient, we find that the system changes its behavior at  $p \approx p_c$ . However, since these changes in the average depend on  $p_n$  and  $p_-$ , we focus our attention in the deviation  $\sigma_m$  of the mean state. This quantity measures how many differ-

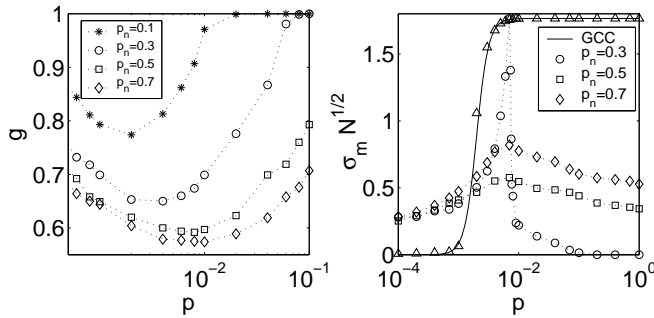


FIG. 4: Left: Dependence of  $g$  with the adding probability  $p$ , in a log-linear scale, for different probabilities  $p_n$ . Each point is an average over 100 different realizations of a  $N = 800$  network. Right: Deviation  $\sigma_m \sqrt{N}$  of the mean state vs.  $p$  for different  $p_n$  values in a log-linear scale, with  $N = 800$ . Each point averages 1000 runs after a transient of 100 iterations and fixed  $p_- = 0.1$ .

ent states are allowed for that particular network structure. It can be seen in Fig. 4(right) that the maximum of  $\sigma_m$  is reached when the GCC associated to the long-range links spans the whole network with a minimal number of links.

This shows how  $p$  and  $p_n$  contribute to improve the synchronization even for this discrete dynamics. When the net is essentially a lattice, the system remains in disorder since there are few  $\lambda_i > 0$  to spread the activity throughout. If we have a fully connected network with many  $\lambda_i > 0$ , the whole system is activated but, since all dimensions in  $S^+$  contribute similarly to the dynamics, the topology constrains the neurons to evolve alike when they have different intrinsic dynamics. On the contrary, the structure close to  $p_c$ , due to the presence of phase-repulsive links is such that, not only the activity is enhanced, but also the topology is compatible with the heterogeneity of the system.

In summary, we have shown how a small fraction of phase-repulsive links can enhance synchronization in a complex network of dynamical units. A structural analysis allows us to obtain information about how the topology influences the dynamics. Surprisingly, around  $p_c$ , the versatility arising from the network structure due to  $p_n$  drives the system to a more ordered state, while far from  $p_c$  the stiffness of the structure freezes the initial disorder.

We thank Dr. J.R. Peláez for fruitful discussions. This work has been financially supported by the Spanish Ministry of Science and Technology under project No. BFM2003-03081 and the URJC project No. PPR2004-04. All numerical computations were performed at the Centro de Apoyo Tecnológico of the Universidad Rey Juan Carlos.

- [2] R. Sergev, M. Benveniste, E. Hulata, N. Cohen, A. Palevski, E. Kapon, Y. Shapira, and E. Ben-Jacob, Phys. Rev. Lett. **88**, 118102 (2002).
- [3] L. C. Jia, M. Sano, P. Lai, and C. K. Chan, Phys. Rev. Lett. **93**, 088101 (2004).
- [4] V. M. Eguiluz, D. R. Chialvo, G. A. Cecchi, M. Baliki, and A. V. Apkarian, Phys. Rev. Lett. **94**, 018102 (2005).
- [5] M. Barahona and L. Pecora, Phys. Rev. Lett. **89**, 05101 (2002).
- [6] S. Strogatz, Nature **410**, 268 (2001).
- [7] R. Albert and A. Barabási, Rev. Mod. Phys. **47**, 74 (2002).
- [8] T. Nishikawa, A. E. Motter, Y.-C. Lai, and F. Hoppensteadt, Phys. Rev. Lett. **91**, 014101 (2003).
- [9] A. E. Motter, C. Zhou, and J. Kurths, Phys. Rev. E **71**, 016116 (2005).
- [10] M. Chavez, C.-U. Hwang, A. Aman, H. Hentschel, and S. Boccaletti, Phys. Rev. Lett. **94**, 218701 (2005).
- [11] L. Lago-Fernández, R. Huerta, F. Corbacho, and J. A. Sugüenza, Phys. Rev. Lett. **84**, 2758 (2000).
- [12] I. Belykh, E. de Lange, and M. Hasler, Phys. Rev. Lett. **94**, 188101 (2005).
- [13] M. I. Rabinovich, P. Varona, A. I. Selverston, and H. D. Abarbanel, Rev. Mod. Phys. (2005), in press.
- [14] G. Balázs, A. Cornell-Bell, A. B. Neiman, and F. Moss, Phys. Rev. E **64**, 041912 (2001).
- [15] L. Tsimring, N. Rulkov, M. Larsen, and M. Gabbay, Phys. Rev. Lett. **95**, 014101 (2005).
- [16] I. Aradi and I. Soltesz, J. Physiol. **538**, 227 (2002).
- [17] A. Hodgkin and A. F. Huxley, J. Physiol. **117**, 500 (1952).
- [18] Parameters:  $C = 1 \mu\text{F}/\text{cm}^2$ ,  $g_{Na} = 120 \text{ mS}/\text{cm}^2$ ,  $g_K = 36 \text{ mS}/\text{cm}^2$ ,  $g_l = 0.3 \text{ mS}/\text{cm}^2$ ,  $V_{Na} = 50 \text{ mV}$ ,  $V_K = -77 \text{ mV}$ ,  $V_l = -54.4 \text{ mV}$ . Functions  $\alpha_x$  and  $\beta_x$  with  $x \in \{m, h, n\}$ :  $\alpha_m = 0.1(V+40)/(1-\exp(-(V+40)/10))$ ;  $\beta_m = 4 \exp(-(V+65)/18)$ ;  $\alpha_h = 0.07 \exp(-(V+65)/20)$ ;  $\beta_h = 1/(1+\exp(-(V+35)/10))$ ;  $\alpha_n = 0.01(V+55)/(1-\exp(-(V+55)/10))$ ;  $\beta_n = 0.125 \exp(-(V+65)/80)$ .
- [19] S. Boccaletti, V. Latora, Y. Moreno, M. Chavez, and D.-U. Hwang, Physics Reports **424**, 175 (2006).
- [20] G. Ermentrout and N. Kopell, SIAM J. Appl. Math. **54**, 478 (1994).
- [21] G. Balázs, A. Cornell-Bell, and F. Moss, Chaos **13**, 515 (2003).
- [22] G. Tanaka, B. Ibarz, M. A. F. Sanjuán, and K. Aihara, Chaos **16**, 013113 (2006).
- [23] L. Pecora and T. Carrol, Phys. Rev. Lett. **80**, 2109 (1998).
- [24] D. J. Watts, *Small Worlds* (Princeton University Press, 1999).
- [25] H. Zhou and R. Lipowsky, Proc. Natl. Acad. Sci. USA **102**, 10052 (2005).

[1] M. R. Mehta, A. K. Lee, and M. A. Wilson, Nature **417**, 741 (2002).